EFFECTS OF CONNECTIVITY DISORDER ON THE POTTS MODEL*

Wolfhard Janke[†] and Martin Weigel[‡]

Institut für Theoretische Physik, Universität Leipzig
Augustusplatz 10/11, 04109 Leipzig, Germany

The relevance of quenched, *uncorrelated* disorder coupling to the local energy density, its paradigm being the random-bond model, is judged by the Harris criterion. A generalization of the underlying argument to the case of spatially *correlated* disorder, exemplified by quasi-crystals, has been given by Luck. We address the question, whether a relevance criterion of this type is applicable to the case of spin models coupled to different kinds of *random graphs*. The geometrical fluctuation exponent appearing in Luck's criterion is precisely determined for the cases of two-dimensional Poissonian Voronoï–Delaunay random lattices and planar, "fat" ϕ^3 Feynman diagrams. While previous work for the latter graphs is in accord with the determined relevance threshold, a preliminary analysis of the results of a Monte Carlo simulation of the three-states Potts model on Poissonian Voronoï lattices presented here does not meet the expectations from the relevance criterion.

PACS numbers: 75.10.Hk, 75.40.Mg, 75.50.Lk

1. Introduction

For the investigation of the effect of quenched disorder on the universal aspects of critical phenomena, models with an uncorrelated, random distribution of couplings have been considered as the main example for the whole field of quenched disorder coupling to the local energy density [1–4]. Depending on the considered quenched distribution of couplings, this includes ferromagnetic random-bond models as well as the qualitatively very different case of spin glasses, where the disorder is augmented by energetic frustration resulting from the inclusion of anti-ferromagnetic couplings [2, 5–11]. Concerning the effect of random bonds on a continuous phase transition, it was

† E-mail: `Wolfhard.Janke@itp.uni-leipzig.de`

‡ E-mail: `Martin.Weigel@itp.uni-leipzig.de`

initially believed that the system might break up into a set of essentially uncoupled subsystems which undergo ordering at different temperatures, thus destroying any sharp phase transition [1,8]. In the meantime, however, renormalization group analyses as well as numerical investigations have been able to convincingly show that, instead, the system can cross over to a new, disorder fixed point signifying a new (model-dependent) universality class with corresponding critical exponents [3, 12–16]. Using phenomenological scaling theory, Harris [8] argued that such a crossover should not occur for systems with a specific-heat exponent $\alpha < 0$. In agreement with the experience from examples such as the random-bond Ising and Potts models it is now widely believed that also the converse should be true, *i.e.*, a crossover *does* occur for systems with $\alpha > 0$ [12, 13, 17]. In the marginal case $\alpha = 0$, realized, *e.g.*, by the random-bond Ising model in two dimensions, the regular critical behavior is merely modified by the appearance of logarithmic corrections [3]. On the other hand, for systems exhibiting a first-order phase transition in the regular case, the introduction of quenched disorder coupling to the local energy density can weaken the transition to second (or even higher) order [11]. While this scenario has been rigorously established for the case of two dimensions and an arbitrarily small amount of disorder [9, 10, 18, 19], the situation for higher-dimensional systems is less clear. For a variety of systems in three dimensions, however, the introduction of a sufficiently strong amount of disorder seems to be able to soften the transition to a continuous one, see, *e.g.* Refs. [20–22].

As soon as the assumption of independence of the disorder degrees of freedom is relaxed, the reasoning of the Harris criterion is no longer applicable as it stands. The existence of spatial correlations leads to a modification of the fluctuations present in "typical" patches of the random system with respect to the behavior expected from the central limit theorem for independent random variables, which is implicitly presupposed by Harris' arguments. Such correlations for a random-bond model have been considered occasionally [23–26] and altered relevance criteria have been proposed [23, 27]. Luck [27] has considered a class of irregular systems not covered by the random-bond paradigm, namely that of quasi-crystalline or aperiodic structures, and formulated a generalized relevance criterion. Although he did not consider systems with connectivity *disorder* such as the random graph models to be considered here, his reasoning should also apply to these cases, as will be shown below. Following his argument, the "break-even point" for relevance of correlated disorder is shifted from the uncorrelated case $\alpha_c = 0$ to somewhere in the interval $-\infty < \alpha_c \leq 1$, depending on a characteristic of the correlations of the disorder variables termed the geometrical fluctuation or *wandering exponent* [27]. Although critical phenomena on lattices subject to connectivity disorder have been considered before by Monte Carlo simu-

lations [28–36] and analytical methods [37–42], to our knowledge no contact has been made with Luck's predictions, and the wandering exponents of the considered random graphs have not yet been taken into account.

In Section 2, we elaborate on a formulation of Luck's relevance criterion appropriate for the considered random graphs and numerically determine the wandering exponents occurring for the classes of two-dimensional Poissonian Voronoï–Delaunay triangulations [43] and the planar ϕ^3 Feynman diagrams of the dynamical triangulations model [44]. Section 3 is devoted to a report on the preliminary results of a high-precision Monte Carlo simulation study of the three-states Potts model on planar, Poissonian Voronoï lattices. Finally, Section 4 contains our conclusions.

2. The Harris–Luck criterion

In the following, we present two examples of classes of random graphs exhibiting spatial correlations of the co-ordination number distributions, which are the disorder degrees of freedom for these lattices. In this respect, these graphs are different from "generic" random graph models [45], where bonds are distributed completely at random between a given number of nodes, such producing uncorrelated connectivity disorder.

2.1. Correlated random graphs of Voronoï–Delaunay type

The planar Voronoï–Delaunay construction [43] prescribes a segmentation of a patch of the plane into convex polygons compatible with a given set of point positions (generators). The Voronoï cell of a generator is defined as the region of the plane, which is closer to it than to any other generator. The three-valent vertices where these cells meet and the cell edges make up the Voronoï graph associated with the generators. Accordingly, the structure geometrically dual to the Voronoï graph is the Delaunay triangulation of the considered patch of the plane. The Voronoï–Delaunay construction for an arbitrary distribution of generators can be considered as a generalization of (and includes as a special case) the Wigner–Seitz elementary cells of regular lattices.

Now, consider the regular cell structure generated by the Voronoï–Delaunay construction from a regular arrangement of points such as, *e.g.*, the vertices of a triangular lattice. The randomness in a physical system to be modeled by this lattice could be accounted for by randomly displacing the generators and re-applying the Voronoï–Delaunay construction to adapt the lattice accordingly. In the limit of large, isotropic displacements this leads to a maximally disordered system with an equal distribution of generators in the region under consideration. The resulting Voronoï–Delaunay graph is referred to as *Poissonian random lattice* since the generators can
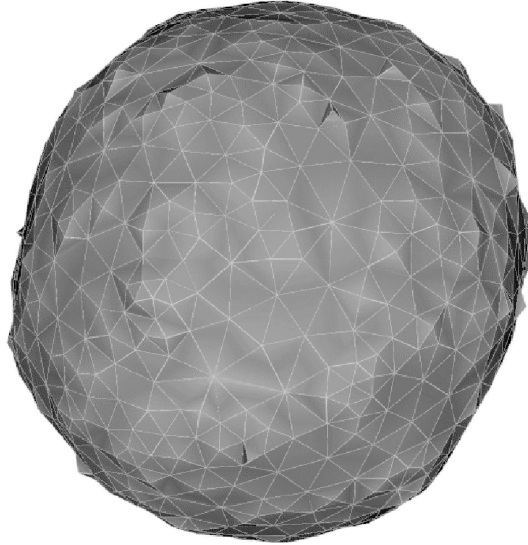
Fig. 1. Snapshot of a Poissonian Voronoï–Delaunay random graph of spherical topology and with $N = 5000$ triangles. The shown triangles constitute the Delaunay tessellation with vertices of varying co-ordination number. The Voronoï graphs considered numerically are the geometric duals of the shown structure.

be considered as realization of a Poisson point process [43, 46]. To eliminate surface effects, the Voronoï–Delaunay construction is applied to generators distributed at random on a sphere. The Delaunay triangulation resulting from such a process is depicted in Fig. 1.

In the resulting Voronoï–Delaunay graph, the disorder appears in the distributions of edge lengths, cell volumes *etc.* and in the random distribution of co-ordination numbers for the Delaunay triangulations resp. the loop length distribution of the dual Voronoï graphs. For the analyses to be presented below, we restrict ourselves to the topological structure of the lattices, *i.e.*, we ignore any length differences and consider only the connectivity structure of the abstract graphs. Hence, variation of co-ordination numbers q_i of the triangulation resp. loop lengths of the dual graph, *i.e. connectivity disorder*, is the only remaining effect of randomness. From the Euler relations, the average co-ordination number is a topological invariant for a fixed number of triangles in two dimensions, given by [44]

$$\bar{q} = \frac{1}{N} \sum_i q_i = 6\frac{N}{N+4}\,, \tag{1}$$

for any closed triangulation, where N denotes the number of triangles. Obviously, one has $\langle\bar{q}\rangle = \langle q_i\rangle = 6$ for $N \to \infty$. The expected variance of

co-ordination numbers can be shown to approach [43, 47]

$$\mu_2 \equiv \langle q_i^2 \rangle - \langle q_i \rangle^2 \approx 1.781 \,, \tag{2}$$

as $N \to \infty$. It turns out that the random variables q_i are not independently distributed, but are reflecting a spatial correlation of the disorder degrees of freedom in addition to the trivial correlation induced by the constraint (1). The form of these correlations for nearest-neighbor vertices is commonly described by the Aboav–Weaire law [43], which states that the total expected number of edges of the neighbors of a q-sided cell, $q\,m(q)$, should vary linearly with q,

$$q\,m(q) = (6 - a)q + b \,, \tag{3}$$

where a and b are some parameters. Equation (3) is a good description for the nearest-neighbor correlations in a large variety of random structures encountered in nature; it can be shown, however, that it applies only approximately in most cases, including that of Poissonian random lattices [46].

2.2. Correlated random graphs of dynamical triangulation type

A different ensemble of random graphs results from the gluing of a fixed number N of equilateral triangles to a closed surface of spherical topology, where all possible gluings are counted with equal probability. This defines
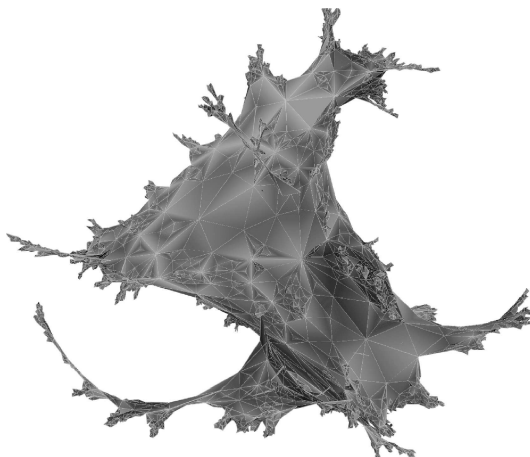

Fig. 2. Snapshot of a dynamical triangulation of volume $N = 5000$ triangles. The considered planar, "fat" ϕ^3 diagrams correspond to the geometric duals of these triangulations.

the *dynamical triangulations* model used as a constructive approach to quantum gravity [44]. The graphs dual to these triangulations are planar, "fat" (*i.e.*, orientable) ϕ^3 Feynman diagrams without tadpoles and self-energy insertions, which can be counted analytically by matrix model methods [44,48]. An example of a dynamical triangulation, embedded in three-dimensional space for illustration purposes, is depicted in Fig. 2. As can be seen, fluctuations are much more pronounced in these structures than in the Poissonian random lattices. In fact, it can be shown that the asymptotic variance of co-ordination numbers is exactly $\mu_2 = 10.5$ [49], whereas Eq. (1) still holds. Comparing the full distributions of co-ordination numbers [47,48,50] shown in Fig. 3, it is seen that for the dynamical triangulations model large co-ordination numbers are much more probable than for the case of Poissonian random lattices. Vertices with large co-ordination number appear at points of the lattice, where "baby universes" branch off from the main surface, *i.e.*, macroscopical subgraphs attached to the main body by only a few links. In fact, the considered graph ensemble can be described as that of (statistically) self-similar, fractal trees of "baby universes" [51]. The "baby universe" structure is reflected in an exceptionally large internal Hausdorff dimension of $d_{\mathrm{h}} = 4$ [52,53] as compared to the dimension $d_{\mathrm{h}} = 2$ of the Poissonian random lattice model. As will be shown below, dynamical triangulations
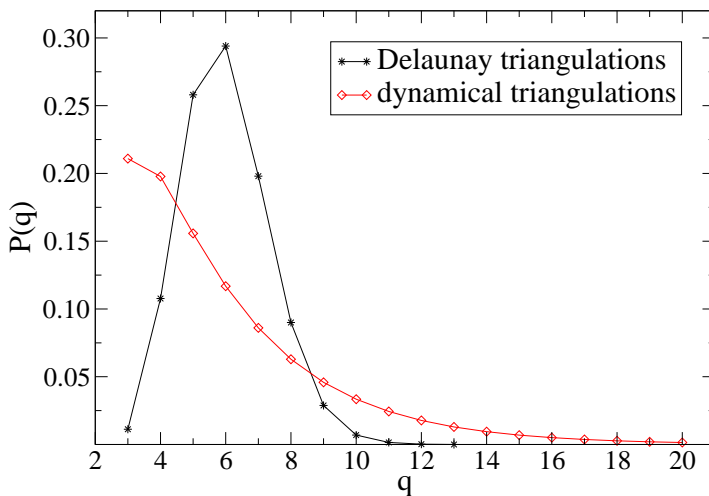

Fig. 3. Comparison of the co-ordination number distributions $P(q)$ of Poissonian Delaunay triangulations and dynamical triangulations in the limit of an infinite number of triangles.

graphs also exhibit spatial correlations between the co-ordination numbers, which are in fact much stronger than those found for Poissonian random lattices.

2.3. Relevance for critical phenomena

According to the argument put forward by Harris [8] and its mathematical backing-up given in Refs. [54, 55], the relevance of randomness coupling to the local energy density crucially depends on how fast fluctuations of the local transition temperature induced by fluctuations of the random variables in a correlation volume die out as the critical point is approached. For independent random variables, this decay occurs with an exponent of $d/2$ in d dimensions. The comparison of this power with the inverse correlation length exponent $1/\nu$ leads to Harris' celebrated relevance criterion.

Following Luck [27], this reasoning can be extended to the correlated random variables present in the random graph models under consideration as follows. Consider a spherical patch P of radius R on a triangulation containing $B(R)$ vertices[1]. Then, the fluctuations of the average co-ordination number in P,

$$J(R) \equiv \frac{1}{B(R)} \sum_{i \in P} q_i \,, \tag{4}$$

around its expected value $J_0 = \bar{q}$ [*cf.* Eq. (1)] in general decays in the limit $R \to \infty$ of large patches as

$$\sigma_R(J) \equiv \frac{\langle |J(R) - J_0| \rangle}{J_0} \sim \langle B(R) \rangle^{-(1-\omega)} \sim R^{-d_{\mathrm{h}}(1-\omega)} \,, \tag{5}$$

defining the wandering exponent ω of the considered graph type. Here, the averages $\langle \cdot \rangle$ are to be understood as the ensemble averages of the considered class of graphs of a given total size. While for $\omega = 1/2$ the usual $1/\sqrt{\langle B(R) \rangle}$ behavior of uncorrelated random variables is recovered, for random lattices with long-range correlations of the co-ordination numbers one expects $\omega > 1/2$, leading to a slowed-down decay of fluctuations. Near criticality, the fluctuation $\sigma_\xi(J)$ of the average co-ordination number in a correlation volume induces a local shift of the transition temperature proportional to $|t|^{d_{\mathrm{h}}\nu(1-\omega)} \mu_2^{1/2}$. For the regular critical behavior to persist, these fluctuations should die out as the critical point $t = 0$ is approached. This is the case when ω does not exceed the threshold value

$$\omega_{\mathrm{c}}(\nu) = 1 - \frac{1}{d_{\mathrm{h}}\nu} = \frac{1 - \alpha}{2 - \alpha} \,, \tag{6}$$

---

[1] All distances on the graphs considered in this paper are to be understood as the number of links in the unique shortest path of links connecting two vertices.

provided that hyper-scaling is applicable. On the other hand, for $\omega > \omega_c(\nu)$ a new type of critical behavior could occur. Re-writing Eq. (6) as

$$\alpha_c = \frac{1 - 2\omega}{1 - \omega}\,, \tag{7}$$

it is obvious that for $\omega = 1/2$ the Harris criterion is recovered.

Since for graphs with sufficiently long-range correlations of the co-ordination numbers $\omega > 1/2$, this type of disorder is *more* relevant than uncorrelated randomness in the sense that a change of universality class can already be expected for some range of *negative* values of α, *cf.* Eq. (7). On the other hand, if correlations decay exponentially, the Harris criterion should stay in effect.

2.4. Determination of wandering exponents

To arrive at predictions for the relevance of the connectivity disorder of the considered classes of graphs to alter the critical behavior of coupled spin systems, we determine the wandering exponent ω numerically by sampling the fluctuations defined in Eq. (5) for a series of graph realizations of the considered ensembles. For the case of the Voronoï–Delaunay graphs the method of generation has been described in Section 2.1; independent realizations of the dynamical triangulations model are generated by a recursive insertion method proposed in Ref. [56]. For both ensembles, an average is taken over 100 different graph realizations. To determine the volume $B(R)$ and the average co-ordination number $J(R)$, a vertex of the triangulation is picked at random and the graph is subsequently decomposed into spherical shells of vertices with link distance R from the chosen origin. The resulting expressions for $B(R)$ and $J(R)$ according to Eq. (4) are then averaged over different choices of origin for each graph and the 100 graph realizations.

The resulting final averaged fluctuations are shown for Voronoï–Delaunay graphs composed of $N = 500\,000$ triangles in Fig. 4 and for dynamical triangulations of $N = 250\,000$ triangles in Fig. 5. Note that the range of accessible distances R for a given number of triangles N is much smaller for the case of dynamical triangulations due to the large fractal dimension $d_h = 4$. According to Eq. (5) these plots should show an approximately linear behavior in a logarithmic presentation for large distances R, the slope of the line being given by $1 - \omega$. For an intermediate range of volumes $B(R)$ and, consequently, distances R, these expectations are met for both graph types. For $1/B(R) - 1/N$ small, however, this behavior is superimposed by an exponential decline of fluctuations. This stems from the topological constraint (1) expressing the absence of fluctuations of the average co-ordination number of the whole graph and is thus a finite-size effect. The appearance of this exponential drop corresponds to the canonical ensemble of a fixed number
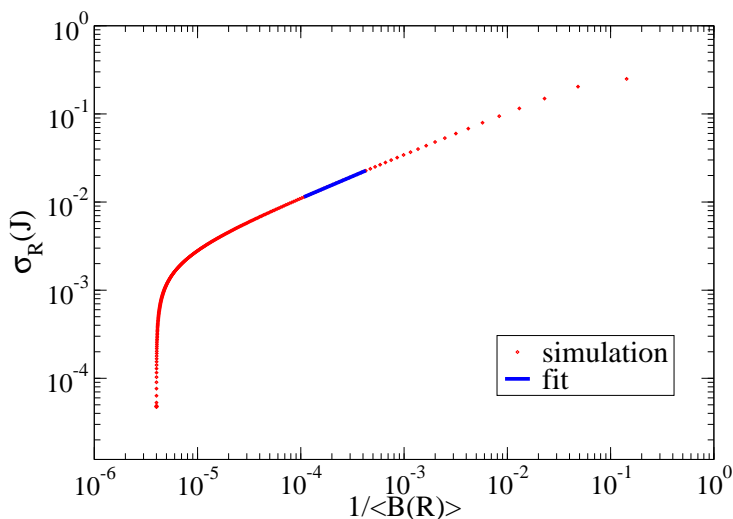
Fig. 4. Numerical estimate of the scaling of the average fluctuation of co-ordination numbers of Voronoï–Delaunay triangulations of volume $N = 500\,000$ and a fit to the expected functional form (5).
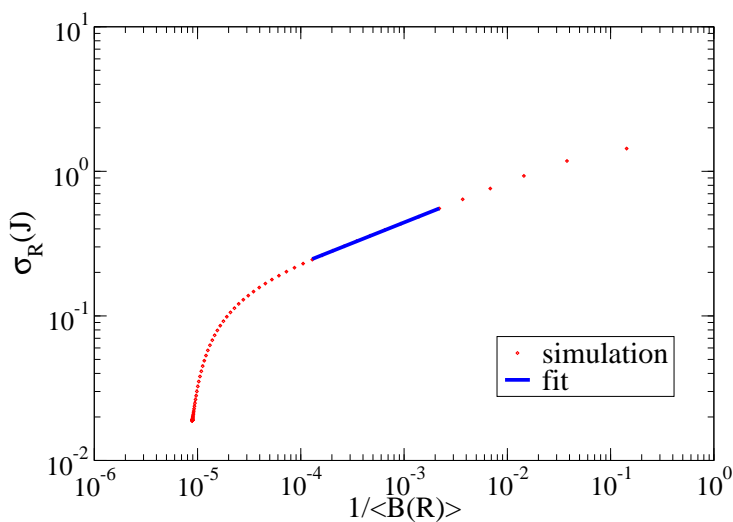

Fig. 5. Scaling of the average fluctuation of co-ordination numbers for combinatorial dynamical triangulations of volume $N = 250\,000$ and a fit to the functional form (5).

of altered or deleted bonds that is sometimes used in the random-bond type model as opposed to the more conventional grand-canonical description with fluctuating numbers of bond species [57–59]. Hence, taking discretization effects for small R into account, only a rather small window of distances can be used for a reliable determination of the wandering exponent via a fit to the functional form (5). This is done by successively dropping events from either side of the range of R's while monitoring the quality-of-fit parameters[2] χ^2 and Q. Taking these considerations into account, our estimate for the wandering exponent for Voronoï–Delaunay triangulations becomes,

$$\omega = 0.50096(55)\,, \tag{8}$$

whereas for dynamical triangulations we arrive at

$$\omega = 0.7155(28)\,. \tag{9}$$

The given error estimates are calculated by jackknifing [60,61] over the whole fitting procedure, such as to avoid any bias induced by the cross-correlations of the $J(R)$ for different R. Due to the large fractal dimension of the dynamical triangulations graphs, we expect systematical finite-size corrections to be much more pronounced there, such that the quoted statistical error probably does not capture the size of the possible total deviation from the asymptotic behavior.

The result for Voronoï–Delaunay graphs is well consistent with $\omega = 1/2$ which would result from correlations decaying with a power larger than $d = 2$ (see also Ref. [23]). A direct inspection of the correlation function of co-ordination numbers indicates an even exponential decay [62]. Thus, the relevance criterion (7) reduces to the Harris criterion; Voronoï–Delaunay connectivity disorder should be a relevant perturbation for models with specific-heat exponent $\alpha > 0$. For the dynamical triangulations, on the other hand, the co-ordination number correlations are found to be algebraic (which is consistent with the results obtained from a direct analysis of the correlation function [62]) and, according to Eq. (7), these graphs should alter the critical behavior of any model with $\alpha \gtrsim -1.5$, *i.e.*, of *all* conventional models.

3. The Potts model on Voronoï diagrams

With the aim of finding altered critical behavior from coupling to the described random lattices, we consider the q-states Potts model [63]. From the determination of wandering exponents presented in the last section we conclude that for the Ising model ($q = 2$, $\alpha = 0$) dynamical triangulations

---

[2] Note that due to the correlations between values of $J(R)$ for different distances R, the *absolute* values of χ^2 resp. Q are not immediately meaningful; relative changes, however, are.

should be a relevant perturbation, whereas Voronoï–Delaunay graphs should at most induce logarithmic corrections with respect to the regular behavior, which might not be easy to resolve. On the other hand, for the $q = 3, 4$ Potts models with $\alpha = 1/3$, $2/3$, respectively, the relevance criterion (7) with the found values of ω predicts a change of critical behavior for both lattices, dynamical triangulations and Voronoï–Delaunay graphs.

Indeed, simulations of the $q = 2, 3, 4$ Potts models coupled to dynamical triangulations provide good evidence for a cross-over to new universality classes [33, 34, 64]. Furthermore, the exact solution of the percolation model, which has $\alpha = -2/3$ and corresponds to the limit $q \rightarrow 1$ of the Potts model, on dynamical triangulations shows a shift to a different universality class [65, 66]. Also, the first-order case $q = 10$ appears to get softened to a continuous transition [67, 68]. On the other hand, simulations of the Ising model on two-dimensional Delaunay triangulations yield Onsager exponents; the presence of possible logarithmic corrections could not be detected [28, 29, 69]. Moreover, the *three-dimensional* Ising model, which has a positive specific-heat exponent $\alpha \approx 0.1$, does not show any crossover to new universal behavior when coupled to Delaunay tessellations in Monte Carlo simulations [35] (however, the wandering exponent for Poissonian random lattices in *three dimensions* has not yet been determined). For the $q = 3$ Potts model in two dimensions only an exploratory study with rather small graphs is available, which does *not* show a change of critical behavior as compared to that on regular lattices [31]. Here, we present the preliminary results of a set of high-precision Monte Carlo simulations of the $q = 3$ Potts model on Voronoï diagrams of up to $N = 80\,000 \approx 280^2$ vertices.

3.1. Model and simulation

We consider the ferromagnetic, zero-field three-states Potts model with Hamiltonian

$$\mathcal{H} = -J \sum_{\langle i,j \rangle} \delta_{s_i s_j}, \tag{10}$$

where $s_i \in \{1, 2, 3\}$ and the sum runs over all nearest-neighbor pairs of vertices of a Voronoï diagram. As has been mentioned above in Section 2.1, we consider the Voronoï graph as a topological object, with equal distances set to unity between any two nearest-neighbor vertices. All simulations are performed using the Swendsen–Wang (SW) cluster algorithm for the Potts model [70] for a fixed realization of the Voronoï graph. The disorder averages are performed on the level of the free energy and its derivatives using 100 different realizations of Voronoï graphs. The sufficiency of this number of replica is checked by performing the same analyses with only half the number of graphs: apart from the expected increase in statistical fluctuations, we

find consistent results from this reduced set of replicas for all quantities considered. By exemplary determination of integrated autocorrelation times using a jackknifing technique [60, 61], we checked that it only takes a few SW updates for all considered graph sizes and temperatures to create an effectively uncorrelated new configuration. For the finite-size scaling analysis to be presented below, simulations were performed for graphs of sizes $N = 1000, 5000, 10\,000, 20\,000, 40\,000, 60\,000$, and $80\,000$. For each replica, after thermalization $50\,000$ measurements were taken, yielding a total statistics of 5×10^6 events per lattice size. To arrive at estimates of the various considered quantities as continuously varying functions of the coupling $K = \beta J$, we make use of the reweighting technique [71, 72].

3.2. Scaling analysis

To determine the full set of critical exponents of the model and the critical coupling $K_c = \beta_c J$, we apply a well tried sequence of finite-size scaling analyses, see, e.g., Refs. [33, 73]. First, to determine the correlation length exponent ν, we make use of the fact that the logarithmic derivatives of the order parameter[3] m as well as the derivative of the Binder cumulant $U = 1 - \langle m^4 \rangle / 3 \langle m^2 \rangle^2$ at their respective maxima should scale as

$$A_{\max}(N) \sim a N^{1/2\nu}(1 + bN^{-\theta/2}),\tag{11}$$

where we restrict ourselves to $A = \mathrm{d}U/\mathrm{d}K$, $A = \mathrm{d}\ln m/\mathrm{d}K$ and $A = \mathrm{d}\ln m^2/\mathrm{d}K$. For the preliminary analysis presented here, we do not take the correction term into account, i.e., we set $b = 0$ throughout. Figure 6 shows the results of the scaling analysis together with fits to the functional form (11). To account for the visible effects of scaling corrections, we include only results for $N \geq 20\,000$. These fits yield,

$$\nu = \begin{cases} 0.8342(46), & A = \frac{\mathrm{d}U}{\mathrm{d}K}, \\ 0.8328(26), & A = \frac{\mathrm{d}\ln m}{\mathrm{d}K}, \\ 0.8340(26), & A = \frac{\mathrm{d}\ln m^2}{\mathrm{d}K}, \end{cases}\tag{12}$$

a weighted average of which gives the final estimate $\nu = 0.8335(46)$. With this estimate of ν, the critical coupling can be found from the peak positions of various observables,

$$K(A_{\max}, N) \sim K_c + aN^{-1/2\nu},\tag{13}$$

with A one of c_V, $\mathrm{d}m/\mathrm{d}K$, $\mathrm{d}\ln m/\mathrm{d}K$, $\mathrm{d}\ln m^2/\mathrm{d}K$, $\mathrm{d}U/\mathrm{d}K$, or χ, where $c_V = K^2 N[\langle e^2 \rangle - \langle e \rangle^2]$ and $\chi = N[\langle m^2 \rangle - \langle m \rangle^2]$, and e denotes the internal

---

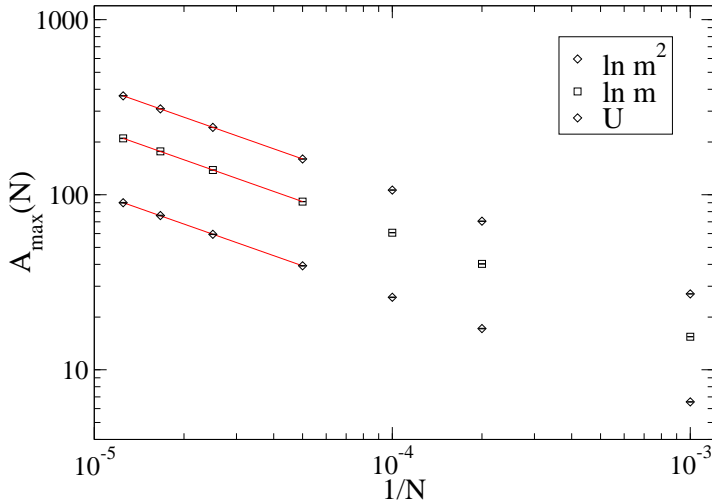[3] To break symmetry explicitly, we use the maximum definition of m, see, e.g. Ref. [74].

Fig. 6. Finite-size scaling of the maximum slope of the Binder parameter U, and the logarithms of magnetization moments $\ln m$ and $\ln m^2$ of the three-states Potts model on Voronoï graphs as a function of the graph size N. The solid lines show fits to the leading term of the functional form (11).

energy per site. An error weighted average of these independent estimates gives $K_c = 1.524\,876(21)$, where the error does not take into account the uncertainty in ν. This value should be compared with the critical coupling of the three-states Potts model on the honeycomb lattice, which is given by $K_c \approx 1.484\,21$ [63].

Further critical exponents are determined independently from the following relations,

$$c_{V,\mathrm{max}}(N) \sim N^{\alpha/2\nu}, \quad m_{\mathrm{inf}}(N) \sim N^{-\beta/2\nu}, \quad \chi_{\mathrm{max}}(N) \sim N^{\gamma/2\nu}, \qquad (14)$$

where m_{inf} denotes the magnetization at its point of inflection. This yields the values $\alpha/2\nu = 0.2201(27)$, $\beta/2\nu = 0.0617(14)$, and $\gamma/2\nu = 0.8718(12)$. To check whether the expected scaling relations are fulfilled and to compare with the exponents of the regular model, we re-write these results in terms of the scaling dimensions x_ϵ and x_σ [75],

$$x_\epsilon = 2 - 2\frac{1}{2\nu} = 1 - \frac{\alpha}{2\nu}, \quad x_\sigma = 2\frac{\beta}{2\nu} = 1 - \frac{\gamma}{2\nu}. \qquad (15)$$

The results for the scaling dimensions together with those of the regular-lattice model are compiled in Table I. The values of x_ϵ from $1/\nu$ seem to match perfectly among the regular and random lattice models, whereas x_ϵ

TABLE I

Results for the scaling dimensions x_ϵ and x_σ of the three-states Potts model on Voronoï graphs as compared to the regular lattice model.

Lattice	$x_\epsilon(1/2\nu)$	$x_\epsilon(\alpha/2\nu)$	$x_\sigma(\beta/2\nu)$	$x_\sigma(\gamma/2\nu)$
Voronoï	0.8003(67)	0.7799(27)	0.1234(27)	0.1282(12)
Regular	0.8000	0.8000	0.133$\bar{3}$	0.133$\bar{3}$

from $\alpha/2\nu$ is significantly differing between the two lattice types. This, however, cannot be taken very seriously, since it is known [73] that direct inspection of the specific heat is usually not well suited for a reliable determination of α. The results for x_σ both differ from the regular lattice value by about four standard deviations. This could be interpreted as the result of neglected corrections to scaling *or* possibly as the onset of a different scaling behavior for even larger lattice sizes.

4. Conclusions

We have analyzed the applicability of a relevance condition in the spirit of the Harris criterion to the case of spin models coupled to random lattices with connectivity disorder. Adapting Luck's formulation [27] for quasiperiodic lattices to the case of random graphs, we numerically determine the geometric wandering exponents of two-dimensional Poissonian Voronoï–Delaunay random graphs and dynamical triangulations. For the dynamical triangulations or quantum gravity graphs, the large wandering exponent indicates that they should form a relevant perturbation for all known models, which is in accord with previous explicit results for the q-states Potts model. On the other hand, correlations between the co-ordination numbers seem to decay exponentially for Poissonian random lattices, such that the adapted relevance criterion reduces to Harris' threshold of $\alpha_c = 0$.

For the three-states Potts model with $\alpha = 1/3$, according to this argument, connectivity disorder from Poissonian random lattices should be relevant. The Monte Carlo scaling analysis presented above yields a thermal scaling exponent in very good agreement with that for the regular lattice model. This is remarkable, since connectivity disorder couples to the local energy density, such that a relevant perturbation is expected to predominantly show up in the energy-related exponents. Whether the small, but significant deviation of the measured magnetic scaling dimension from the regular lattice value indicates the onset of a crossover to a new universality class or is merely an effect of neglected corrections to scaling, has to be checked by a more careful scaling analysis including corrections, possibly

augmented by simulations for even larger lattices. Furthermore, models with larger values of the specific-heat exponent α, such as the $q = 4$ Potts model or the Baxter–Wu model [76], which both have $\alpha = 2/3$, might be good candidates to check whether a change of critical behavior can be induced at all by Poissonian random lattices.

REFERENCES

[1] J.L. Cardy, *Scaling and Renormalization in Statistical Physics*, Cambridge University Press, Cambridge 1996.

[2] A.P. Young ed., *Spin Glasses and Random Fields*, World Scientific, Singapore 1997.

[3] B.N. Shalaev, *Phys. Rep.* **237**, 129 (1994).

[4] B. Berche, C. Chatelain, `cond-mat/0207421`, to appaer in *Order, Disorder and Criticality*, ed. Y. Holovatch, World Scientific, Singapore 2003.

[5] M. Mézard, G. Parisi, M.A. Virasoro, *Spin Glass Theory and Beyond*, World Scientific, Singapore 1987.

[6] K.H. Fisher, J.A. Hertz, *Spin Glasses*, University Press, Cambridge 1991.

[7] K. Binder, A.P. Young, *Rev. Mod. Phys.* **58**, 801 (1986).

[8] A.B. Harris, *J. Phys. C* **7**, 1671 (1974).

[9] Y. Imry, M. Wortis, *Phys. Rev.* **B19**, 3580 (1979).

[10] M. Aizenman, J. Wehr, *Phys. Rev. Lett.* **62**, 2503 (1989).

[11] J.L. Cardy, *Physica A* **263**, 215 (1999).

[12] A.W.W. Ludwig, *Nucl. Phys.* **B285**, 97 (1987).

[13] A.W.W. Ludwig, J.L. Cardy, *Nucl. Phys.* **B285**, 687 (1987).

[14] H.G. Ballesteros, L.A. Fernández, V. Martín-Mayor, A. Muñoz Sudupe, G. Parisi, J.J. Ruiz-Lorenzo, *Phys. Rev.* **B58**, 2740 (1998).

[15] P.-E. Berche, C. Chatelain, B. Berche, W. Janke, *Comput. Phys. Commun.* **147**, 427 (2002).

[16] M. Hellmund, W. Janke, *Comput. Phys. Commun.* **147**, 435 (2002).

[17] A.W.W. Ludwig, *Nucl. Phys.* **B330**, 639 (1990).

[18] K. Hui, A.N. Berker, *Phys. Rev. Lett.* **62**, 2507 (1989).

[19] K. Hui, A.N. Berker, *Phys. Rev. Lett.* **63**, 2433 (1989).

[20] H.G. Ballesteros, L.A. Fernández, V. Martín-Mayor, A. Muñoz Sudupe, G. Parisi, J.J. Ruiz-Lorenzo, *Phys. Rev.* **B61**, 3215 (2000).

[21] C. Chatelain, B. Berche, W. Janke, P.-E. Berche, *Phys. Rev.* **E64**, 036120 (2001).

[22] M. Hellmund, W. Janke, *Phys. Rev.* **E67**, 026118 (2003).

[23] A. Weinrib, B.I. Halperin, *Phys. Rev.* **B27**, 413 (1983).

[24] V.V. Prudnikov, A.A. Fedorenko, *J. Phys. A* **32**, L399 (1999).

[25] P.T. Muzy, A.P. Vieira, S.R. Salinas, *Phys. Rev.* **E65**, 046120 (2002).

[26] V. Blavatska, C. von Ferber, Y. Holovatch, cond-mat/0301383.

[27] J.M. Luck, *Europhys. Lett.* **24**, 359 (1993).

[28] W. Janke, M. Katoot, R. Villanova, *Phys. Lett.* **B315**, 412 (1993).

[29] W. Janke, M. Katoot, R. Villanova, *Phys. Rev.* **B49**, 9644 (1994).

[30] W. Janke, R. Villanova, *Phys. Lett.* **A209**, 179 (1995).

[31] F.W.S. Lima, U.M.S. Costa, M.P. Almeida, J.S. Andrade, *Eur. Phys. J.* **B17**, 111 (2000).

[32] F.W.S. Lima, J.E. Moreira, J.S. Andrade Jr., U.M.S. Costa, *Physica A* **283**, 100 (2000).

[33] W. Janke, D.A. Johnston, *Nucl. Phys.* **B578**, 681 (2000).

[34] W. Janke, D.A. Johnston, *J. Phys. A* **33**, 2653 (2000).

[35] W. Janke, R. Villanova, *Phys. Rev.* **B66**, 134208 (2002).

[36] F. Iglói, L. Turban, *Phys. Rev.* **E66**, 036140 (2002).

[37] V.G. Knizhnik, A.M. Polyakov, A.B. Zamolodchikov, *Mod. Phys. Lett.* **A3**, 819 (1988).

[38] F. David, *Mod. Phys. Lett.* **A3**, 1651 (1988).

[39] J. Distler, H. Kawai, *Nucl. Phys.* **B321**, 509 (1989).

[40] W. Janke, D.A. Johnston, *Phys. Lett.* **B460**, 271 (1999).

[41] M.E.J. Newman, D.J. Watts, *Phys. Lett.* **A263**, 341 (2000).

[42] C. Moore, M.E.J. Newman, *Phys. Rev.* **E62**, 7059 (2000).

[43] A. Okabe, B. Boots, K. Sugihara, S.N. Chiu, *Spatial Tessallations — Concepts and Applications of Voronoi Diagrams*, Wiley, New York 2000.

[44] J. Ambjørn, B. Durhuus, T. Jonsson, *Quantum Geometry — A Statistical Field Theory Approach*, Cambridge University Press, Cambridge 1997.

[45] R. Albert, R.-L. Barabási, *Rev. Mod. Phys.* **74**, 47 (2002).

[46] G. Schliecker, *Adv. Phys.* **51**, 1319 (2002).

[47] J.M. Drouffe, C. Itzykson, *Nucl. Phys.* **B235**, 45 (1984).

[48] E. Brézin, C. Itzykson, G. Parisi, J.-B. Zuber, *Commun. Math. Phys.* **59**, 35 (1978).

[49] C. Godréche, I. Kostov, I. Yekutieli, *Phys. Rev. Lett.* **69**, 2674 (1992).

[50] D.V. Boulatov, V.A. Kazakov, I.K. Kostov, A.A. Migdal, *Nucl. Phys.* **B275**, 641 (1986).

[51] S. Jain, S.D. Mathur, *Phys. Lett.* **B286**, 239 (1992).

[52] H. Kawai, N. Kawamoto, T. Mogami, Y. Watabiki, *Phys. Lett.* **B306**, 19 (1993).

[53] Y. Watabiki, *Nucl. Phys.* **B441**, 119 (1995).

[54] J.T. Chayes, L. Chayes, D.S. Fisher, T. Spencer, *Phys. Rev. Lett.* **57**, 2999 (1986).

[55] J.T. Chayes, L. Chayes, D.S. Fisher, T. Spencer, *Commun. Math. Phys.* **120**, 501 (1989).

[56] M.E. Agishtein, A.A. Migdal, *Nucl. Phys.* **B350**, 690 (1991).

[57] F. Pázmándi, R.T. Scalettar, G.T. Zimányi, *Phys. Rev. Lett.* **79**, 5130 (1997).

[58] A. Aharony, A.B. Harris, S. Wiseman, *Phys. Rev. Lett.* **81**, 252 (1998).

[59] M.I. Marqués, J.A. Gonzalo, *Phys. Rev.* **E65**, 057104 (2002).

[60] B. Efron, *The Jackknife, the Bootstrap and Other Resampling Plans*, Society for Industrial and Applied Mathematics [SIAM], Philadelphia 1982.

[61] B. Efron, R.J. Tibshirani, *An Introduction to the Bootstrap*, Chapman and Hall, Boca Raton 1998.

[62] M. Weigel, W. Janke, to be published.

[63] F.Y. Wu, *Rev. Mod. Phys.* **54**, 235 (1982).

[64] A. Wernecke, W. Janke, D. Johnston, to be published.

[65] V.A. Kazakov, *Mod. Phys. Lett.* **A4**, 1691 (1989).

[66] G. Harris, *Nucl. Phys.* **B418**, 278 (1994).

[67] C.F. Baillie, W. Janke, D.A. Johnston, *Phys. Lett.* **B388**, 14 (1996).

[68] C.F. Baillie, W. Janke, D.A. Johnston, *Nucl. Phys. (Proc. Suppl.)* **B53**, 732 (1997).

[69] D. Espriu, M. Gross, P.E.L. Rakow, J. Wheater, *Nucl. Phys.* **B265**, 92 (1986).

[70] R.H. Swendsen, J.-S. Wang, *Phys. Rev. Lett.* **58**, 86 (1987).

[71] A.M. Ferrenberg, R.H. Swendsen, *Phys. Rev. Lett.* **61**, 2635 (1988).

[72] A.M. Ferrenberg, R.H. Swendsen, *Phys. Rev. Lett.* **63**, 1658(E) (1989).

[73] A.M. Ferrenberg, D.P. Landau, *Phys. Rev.* **B44**, 5081 (1991).

[74] M. Weigel, W. Janke, C.-K. Hu, *Phys. Rev.* **E65**, 036109 (2002).

[75] M. Henkel, *Conformal Invariance and Critical Phenomena*, Springer, Berlin/Heidelberg/New York 1999.

[76] R.J. Baxter, *Exactly Solved Models in Statistical Mechanics*, Academic Press, London 1982.